Proceedings of the 7th International Conference on Civil Structural and Transportation Engineering (ICCSTE'22)
Niagara Falls, Canada – June 05-07, 2022
Paper No. 215
DOI: 10.11159/iccste22.215

Experimental Study of the Evolution of the Breach and the Discharge through the Breach Resulting from Piping due to Seepage at the Earth-Fill Dam Bottom

Mehmet Sukru Guney[1], Emre Dumlu[2], Merve Okan[1], Aslı Bor[1], Pelin Aklık[1], Gökmen Tayfur[2]
[1]İzmir University of Economics
Sakarya Caddesi, No:156
35330 Balçova, Izmir, Turkey
sukru.guney@ieu.edu.tr; merve.okan@ieu.edu.tr; asli.turkben@ieu.edu.tr; pelin.aklik@ieu.edu.tr
[2]İzmir Institute of Technology
Gülbahçe Campus 35430 Urla, Izmir, Turkey,
emredumlu@iyte.edu.tr, gokmentayfur@iyte.edu.tr

Abstract - Piping is one of the main causes of the earth-fill dam failures. Most of the researchers realizing numerical analyses make some simplified assumptions concerning the shape of the breach and the discharge of water flowing through the breach. The aim of this study is to realize experiments to provide data needed to perform numerical analyses by making more realistic assumptions. The dam having a height of 0.6 m, a bottom width of 2 m and a crest width of 0.20 m is built in a channel 1 m wide, 0.81 m high and 6.14 m long. The evolution of the breach and the discharge through the breach resulting from piping due to seepage at the earth-fill dam bottom was investigated experimentally. The evolution of the dam failure is recorded by six cameras located at different locations. The time-varied of the breach areas at upstream and downstream sides are determined by applying the Gauss Area functions. The discharge of water through the breach and average outflow velocity are determined by using the continuity equation.

***Keywords*:** Earth-fill dam, Piping, Breach geometry, Breach development, Discharge through breach

1. Introduction

Piping is one of main causes of earth-fill dam failures. Soil erosion in earth structures, particularly in earth dams and levees, might occur through embankment, foundation or from embankment to foundation. This kind of erosion has phases: a) initiation and continuation of erosion, b) progression to form a pipe, and c) formation of a breach [1]. The evolution of breach resulting from piping is an important issue in experimental and numerical investigation concerning embankment dam failure. The FP5 IMPACT (Investigation of Extreme Flood Process and Uncertainty) European project (2001-2004) addressed the assessment and reduction of risks from extreme flooding caused by natural events or the failure of dams and flood defence structures [2]. Research had been undertaken through a combination of laboratory physical modelling, field data collection, field testing, theoretical studies and numerical simulations. There have been many studies about dam failures especially because of overtopping in the literature, however since it is really difficult to observe erosion process and conduct controlled experiments, there are not too much survey about dam failure due to piping [3]–[5]. Chen et al. [4] indicated that between 1954 and 2018, 3541 dam breach accidents occurred and more than 30% of them was due to piping. Greco et al. [6] simulated the evolution of a breach in an earth-dam by means of a two-dimensional depth-averaged (2DH) numerical model, from both the conceptual and the numerical point of view. They also claimed that the strong unsteadiness of the evolution for a dynamical description of the between flow and sediment, since they may be conveyed under non-equilibrium conditions. Sharif et al. [3] constructed a dam 15 cm high in a laboratory flume by using a mixture of sand, silt, and clay with different compaction rates and examined the changes in the depth, area, and volume of erosion during the piping evaluation by utilizing an image processing technique. Most of the researchers realizing numerical analyses make some simplified assumptions concerning shape of a breach and discharge of water flowing through the breach. Morris et al. [7] revealed that instead of simplified approaches, more realistic approaches are required about the breach mechanism as well as the breach geometry and flow through the breach. Zhu et al. [8] investigated experimentally the breaching of

embankments. ASCE/EWRI Task Committee [9] made a publication about earthen embankment breaching (2011). Froehlich [10] presented two nonlinear mathematical models to predict peak discharge. Wang et al. [11] proposed empirical and semi-analytical models for predicting peak outflows caused by embankment dam failures. Ashraf et al. [12] studied the breach parameters by using large scale physical modelling and statistical methods. Tian et al. [13] investigated experimentally formation and evolution characteristics of dam breach and tailing flow from dam failure.

This study is a part of a project supported by the Scientific and Technological Research Council of Turkey. The aim of this project is first to perform piping experiments on dam bodies and then evaluate the experimental findings by using the software package PLAXIS-3D.

2. Experimental Procedure

Dam was built in a rectangular channel 1 m wide, 0.81 m high and 6.14 m long, as shown in Fig.1. Dam body has a height of 0.6 m, a bottom width of 2 m and a crest width of 0.20 m. The slopes of the upstream and downstream sides were equal to 1:1.5, as shown in Fig.1. Water circulates between the lower reservoir and the upper channel by means of a pump. Before the construction of the dam, some common soil mechanics tests were carried out. The dam was constructed by using a mixture consisting of 85 % sand and 15 % clay. The grain- size distribution of the mixture obtained from wet sieve and hydrometer analysis is given in Fig.2.

Fig. 1: Experimental Setup

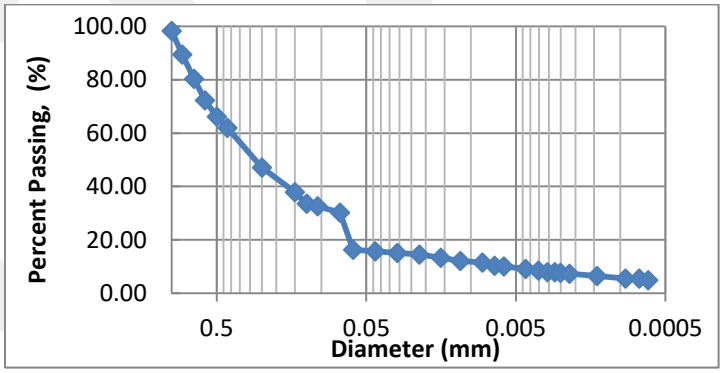

Fig. 2: Grain size distribution of soil with 85% sand and 15% clay

From Figure 2, some characteristic diameters were obtained as D_{10}= 0.006 mm, D_{30}= 0.057 mm, D_{50}= 0.099 mm, and D_{60}= 0.3 mm. The uniformity coefficient C_u equals 54.5 and the curvature coefficient C_c is equal to 1.969.

The specific weight of the mixture was found to be as G_s = 2.63, from the test ASTM D854 – 14.

The permeability of the mixture was found as k= 4.66×10^{-4} cm/s from the falling head permeability test.

From the direct shear test, it was found that the soil has a cohesion value of 15.33 kPa and an internal friction angle of 33.93º.

According to the consolidation test results, the compression index (C_c), recompression index (C_r) and swelling index (C_s) were found to be as 0.100, 0.009 and 0.007, respectively. The oedometric modulus of deformation (E_{oed}) was obtained obtained as 35714 kN/m².

In order to specify the water content, the standard proctor test (ASTM-698) was executed by applying 13 drops and the the so obtained curve is plotted in Figure 3. The reason of applying reduced energy by 50% (13 drops instead of 25) was to increase the probability of the piping occurrence. The maximum dry density and optimum water content were obtained as Υ_{drymax}= 1.794 g/cm^3 and w_{opt} = 12.5 %. The void ratio (e) was calculated as 0.469.

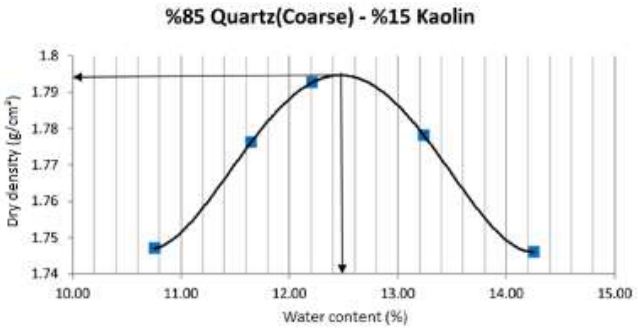

Fig. 3: Dry density – water content relationship

In order to initiate piping resulting from the seepage at the bottom of the earth-fill dam, a layer of cross-section 5 cm by 5 cm was filled by rock salt along the dam axis. The other parts were constructed layer by layer. Each layer of 3.5 cm was compacted so that its thickness becomes 2.5 cm by using Proctor Hammer and 46x92 cm^2 plate. The number of drops were 22. Some construction stages are given in Fig.4.

(a) (b) (c)

Fig. 4: Some construction stages: (a) Filling the 5x5 weak layer by rock salt, (b) Compacting by Proctor Hammer, (c) After the compaction of the second layer

The views corresponding to the finished shape of the dam body are given in Fig.5

(a) (b) (c)

Fig. 5: Views of the final shape of the earth-fill dam, from: (a) Upstream, (b) Downstream, (c) Left side

The flow rate was measured by means of a magnetic flowmeter. The evolution of the dam failure was recorded by cameras located at different locations. Water was pumped from the lower reservoir to upper channel. The water level adjusted by means of an electromagnetic sensor so that the pump starts and stops when water depth in the channel was m and 0.555 m, respectively.

3. Experimental Findings

Once the construction of the dam body was completed, water was supplied to the channel until the water depth reached 55.5 cm. The seepage began after the dissolution of the rock salt. Nevertheless, the formation of the breach occurred much more later. The arrival of the breach at upstream side took about ten days.

The developments of the breach which were recorded by the cameras located at downstream and upstream parts of the dam are given in Fig. 6 and Fig.7, respectively.

(a) (b) (c)

Fig. 6: The temporal development of the breach at downstream a) t=0 h, b) t=48 h, c) t= 230 h

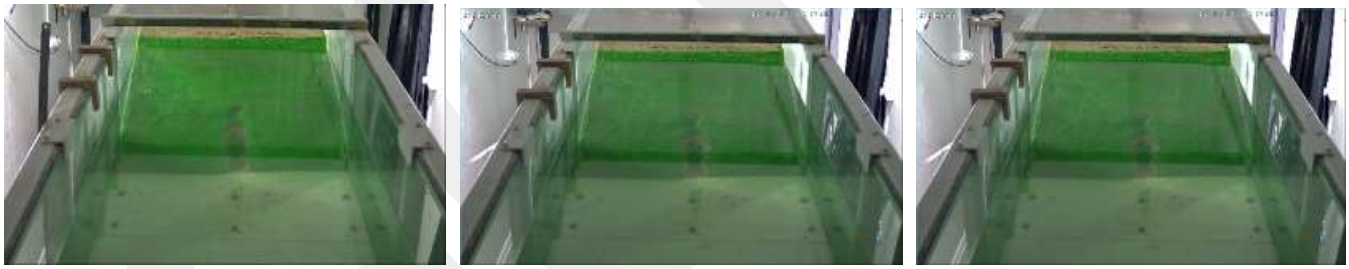

(a) (b) (c)

Fig. 7: The temporal development of the breach at the upstream (a) t=0 h, (b) t=48 h, (c) 230 h

The temporal development of the breach at the downstream and upstream parts are given in Fig. 8 and Fig. 9, respectively. The time t=0 corresponds to the time at which the breach appeared at upstream face.

(a) (b) (c)

Fig. 8: The temporal development of the breach at the downstream (a) t=0 s, (b) t=5 s, (c) 15 s

(d) (e) (f)

Fig.8 (continued): The temporal development of the breach at the downstream (d) 25 s, (e) 60 s, (f) 315 s

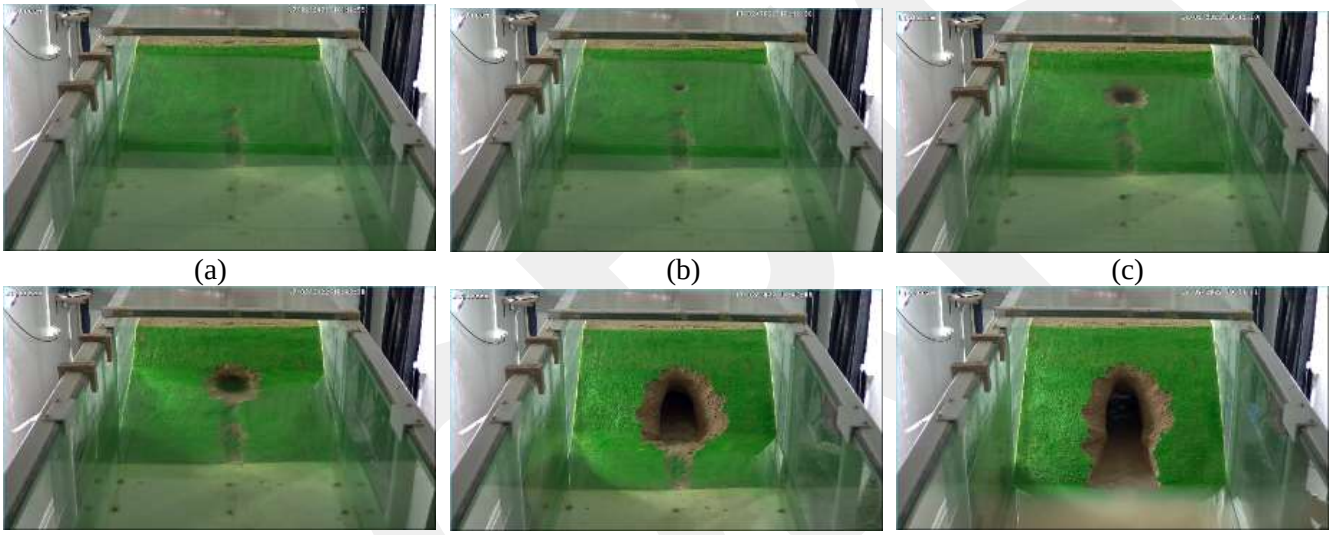

(a) (b) (c)

(d) (e) (f)

Fig. 9: The temporal development of the breach at the upstream (a) t=0 s, (b) t=5 s, (c) 15 s, (d) 25 s, (e) 60 s, (f) 315 s

As seen from Fig. 10, until the arrival of the breach at upstream face, the measured seepage discharges were very low.

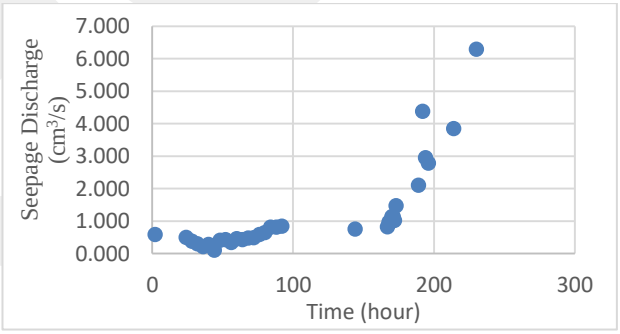

Fig. 10: The seepage discharges when the breach didn't reach the upstream face

From the camera recordings, the water depths in the channel were obtained, and the upstream and downstream cameras images were used to get the shape of the breach and calculate the changes in its geometry. Since the side camera recordings were fish-eye, the videos were straightened using the Hitfilm-Express version 2021.1. Extra sensitive solutions were applied to ensure that the image was completely flat. By using the Get data Graph Digitizer 2.26, the snapshots were scaled and the

boundary coordinates of the breaches in the downstream and upstream sides were determined. The surface areas of the breach were calculated by applying the Gauss Area functions.

The temporal variations of the breach areas at the upstream and downstream and time-dependent discharges through breach, Q_{breach}, are shown in Fig.11.

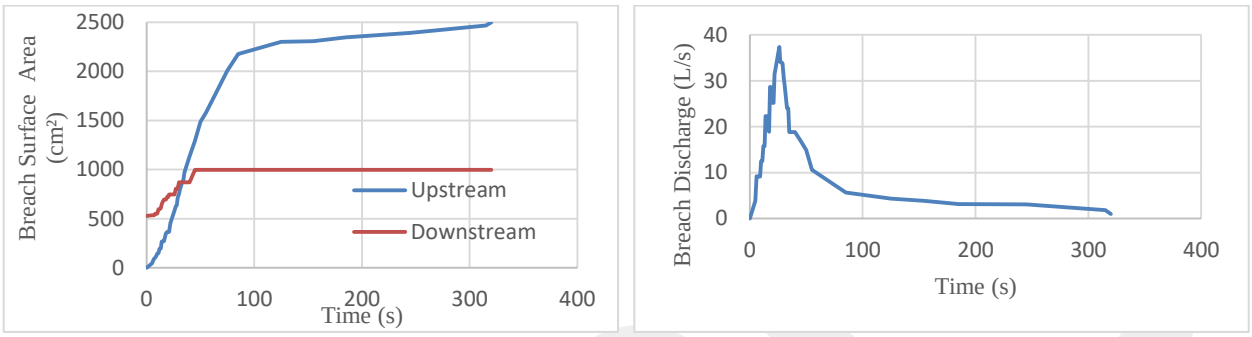

(a) (b)

Fig. 11: a) The temporal variations of the breach surface area at downstream and upstream, b) discharges

The discharge of water through the breach was determined by using the continuity equation, as follows:

$$\Delta S = (Q_{pump} - Q_{breach}) \cdot \Delta t \tag{1}$$

where Q_{pump} is the flow rate delivered by the pump, Q_{breach} is the discharge through the breach, ΔS is the storage in the channel during the time interval Δt.

The average velocity V of the flow through the breach was approximately calculated as follows:

$$V = Q_{breach}/A \tag{2}$$

where A, denotes wetted area.

The temporal variations of the wetted breach areas at the upstream and downstream and corresponding water depths h(t) in the channel are given in Fig.12.

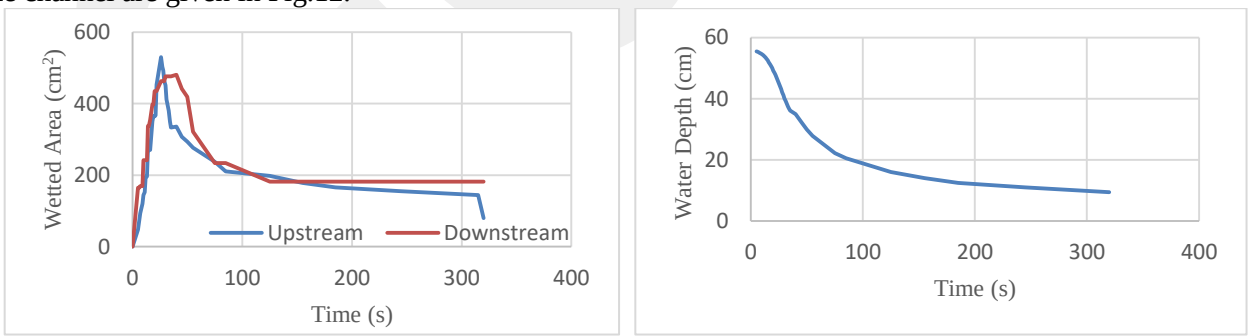

(a) (b)

Fig.12: a) The temporal variations of the wetted area, b) Corresponding water depths in the channel

The so obtained time-varied velocities are plotted in Fig.13.

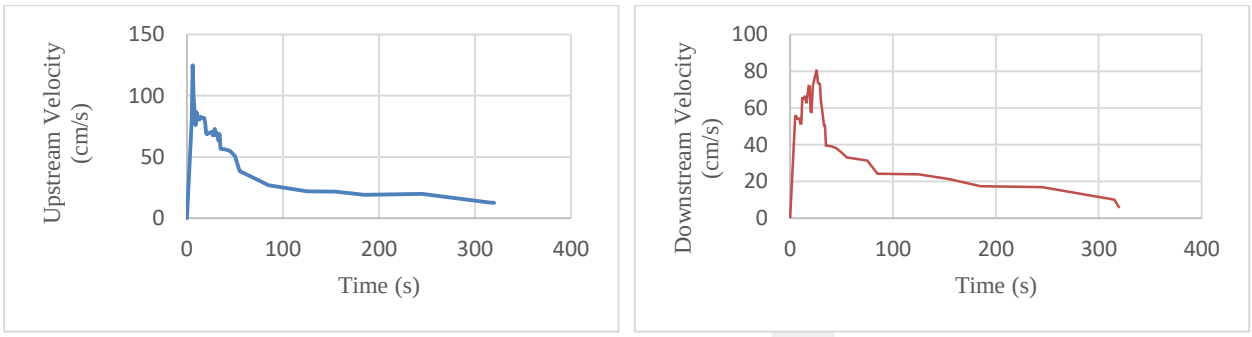

(a) (b)

Fig.13: Time-varied average velocity through the breach at; a) Upstream, b) Downstream

4. Conclusion and Discussion

In this study, time-varied evolution of the breach resulting from the piping at the bottom of earth-fill dam was investigated experimentally. Recordings taken in high resolution were flattened using the Hit-film Express 2021.1. The discharges through the breach at corresponding different time intervals were calculated using the continuity equation. The boundary coordinates of the breach surface areas and wet areas of the breach were obtained using the Get-Data Graph Digitizer, and the areas at each time were calculated by applying the Gauss-area function of these obtained coordinates. The velocity values through the breach areas at corresponding time interval were also calculated. During the experiment, it was observed that the breach started on the downstream side and developed toward the upstream side. The maximum discharge through the breach was calculated as Q_{breach} = 37. 4 L/s at t = 26 s. The breach surface area of the upstream was recorded a maximum level of A_{ups}=2498.7 cm^2 at t=320 s, while downstream A_{down}= 995.99 cm^2 at t=40 s and remained unchanged afterwards. Maximum wetted area was found to be $A_{wetted\text{-}ups}$= 530.18 cm^2 at t= 26 s and $A_{wetted\text{-}downs}$=480.89 cm^2 at t = 40 s, respectively. The maximum velocity values through the breach were calculated as V_{ups}=124.85 cm/s at t= 6 s and V_{down}= 80.86 cm/s at t = 26 s. The pump was turned off at t=315 s, and the experiment was terminated.

In addition to the experimental studies, the numerical analysis also continues to be performed by using the software PLAXIS-3D. It is also aimed to give comments of these experimental findings in the light of the numerical analysis results during the oral presentation.

Acknowledgements

The authors thank the Scientific and Technological Research Council of Turkey (TUBITAK) for supporting the project financially through the project 119M609.

References

[1] R. Fell, C. H. Wan, and M. Foster, “Progress report on methods for estimating the probability of failure of embankment dams by internal erosion and piping,” University of New South Wales, Sydney, Australia, 2003.

[2] Y. Zech and S. Soares-Frazão, “Dam-break flow experiments and real-case data. A database from the European IMPACT research,” *J. Hydraul. Res.*, vol. 45, no. SPEC. ISS., pp. 5–7, 2007.

[3] Y. A. Sharif, M. Elkholy, M. Hanif Chaudhry, and J. Imran, “Experimental Study on the Piping Erosion Process in Earthen Embankments,” *J. Hydraul. Eng.*, vol. 141, no. 7, p. 04015012, 2015.

[4] S. shui Chen, Q. ming Zhong, and G. ze Shen, “Numerical modeling of earthen dam breach due to piping failure,” *Water Sci. Eng.*, vol. 12, no. 3, pp. 169–178, 2019.

[5] M. Elkholy, Y. A. Sharif, M. H. Chaudhry, and J. Imran, “Effect of soil composition on piping erosion of earthen levees,” *J. Hydraul. Res.*, vol. 53, no. 4, pp. 478–487, 2015.

[6] M. Greco, M. Pontillo, M. Iervolino, and A. Leopardi, “2DH numerical simulation of breach evolution in an earth dam,” in *River-flow2008*, 2008, vol. 1, pp. 661–667.

[7] M. Morris, M. Hassan, A. Kortenhaus, P. Geisenhainer, P. Visser, and Y. Zhu, “Modelling breach initiation and growth,” *Flood Risk Manag. Res. Pract.*, pp. 581–591, Oct. 2008.
[8] Y. Zhu, P. J. Visser, J. K. Vrijling, and G. Wang, “Experimental investigation on breaching of embankments,” *Sci. China Technol. Sci.*, vol. 54, no. 1, pp. 148–155, 2011.
[9] The ASCE/EWRI Task Committee on Dam/Levee Breaching (Break Fluvial Processes). / Earthen embankment breaching. In: Journal of Hydraulic Engineering. 2011 ; Vol. 137, No. 12. pp. 1549-1564.
[10] D. C. Froehlich, “Predicting Peak Discharge from Gradually Breached Embankment Dam,” *J. Hydrol. Eng.*, vol. 21, no. 11, pp. 04016041_1 - 04016041_15, 2016.
[11] B. Wang, Y. Chen, C. Wu, Y. Peng, “Empirical and semi-analytical models for predicting peak outflows caused by embankment dam failures,” *J. Hydrol.*, vol. 562, no. May, pp. 692–702, 2018.
[12] M. Ashraf, A. H. Soliman, E. El-Ghorab, and A. El Zawahry, “Assessment of embankment dams breaching using large scale physical modeling and statistical methods,” *Water Sci.*, vol. 32, no. 2, pp. 362–379, 2018.
[13] S. Tian, X. Dai, G. Wang, Y. Lu, and J. Chen, “Formation and evolution characteristics of dam breach and tailings flow from dam failure: an experimental study,” *Nat. Hazards*, vol. 107, no. 2, pp. 1621–1638, 2021.